



## Characteristics of atmospheric PM<sub>2.5</sub> composition during the implementation of stringent pollution control measures in Shanghai for the 2016 G20 summit



Haiwei Li <sup>a</sup>, Dongfang Wang <sup>b</sup>, Long Cui <sup>a</sup>, Yuan Gao <sup>c</sup>, Juntao Huo <sup>b</sup>, Xinning Wang <sup>b</sup>, Zhuozhi Zhang <sup>a</sup>, Yan Tan <sup>a</sup>, Yu Huang <sup>d</sup>, Junji Cao <sup>d</sup>, Judith C. Chow <sup>e</sup>, Shun-cheng Lee <sup>a,\*</sup>, Qingyan Fu <sup>b,\*</sup>

<sup>a</sup> Department of Civil and Environmental Engineering, The Hong Kong Polytechnic University, Hung Hom, Hong Kong

<sup>b</sup> Shanghai Environmental Monitoring Center, Shanghai, China

<sup>c</sup> Chu Hai College of Higher Education, Tuen Mun, Hong Kong

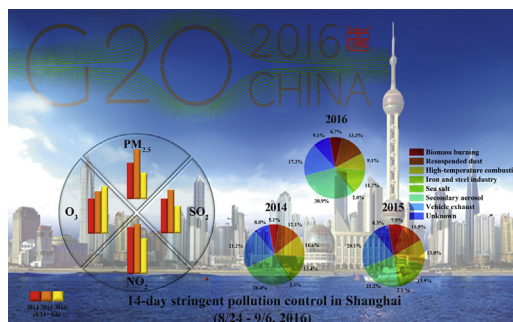
<sup>d</sup> Key Laboratory of Aerosol Chemistry and Physics, Institute of Earth Environment, Chinese Academy of Sciences, Xi'an 710061, China

<sup>e</sup> Division of Atmospheric Sciences, Desert Research Institute, Reno, NV, USA

### HIGHLIGHTS

- Effectiveness of the pollution control measures was evaluated for the G20 summit.
- Concentrations of most of criteria air pollutants reduced whereas O<sub>3</sub> elevated.
- Impacts of local emissions and regional transport were analyzed at two Supersites.
- Secondary aerosols and vehicle exhaust remained the top two sources of PM<sub>2.5</sub>.

### GRAPHICAL ABSTRACT



### ARTICLE INFO

#### Article history:

Received 2 July 2018

Received in revised form 16 August 2018

Accepted 17 August 2018

Available online 18 August 2018

Editor: Jianmin Chen

#### Keywords:

PM<sub>2.5</sub> composition

Pollution control measures

G20 summit

Shanghai

### ABSTRACT

To reduce air pollution within a 300 km radius from Hangzhou (the capital city of Zhejiang Province in East China) for the 2016 G20 summit (9/4–9/5), the 14-day (8/24–9/6) stringent pollution control measures were implemented in Shanghai. Changes in atmospheric concentrations during the same 14-day period from 2014 to 2016 were examined at two Supersites, i.e., urban Pudong site (PD) and Dianshan Lake regional site (DSL). Up to 50% reductions were found for PM<sub>2.5</sub>, with 13.1% and 9.7% reductions for SO<sub>2</sub> and NO<sub>2</sub>, respectively. No apparent improvements were found for 8-h average O<sub>3</sub> concentrations. Large reductions were also found for SO<sub>4</sub><sup>2-</sup> (51.4%), NO<sub>3</sub><sup>-</sup> (68.8%), and NH<sub>4</sub><sup>+</sup> (84.4%), on average. Elevated coefficient of divergence values (0.52–0.56) suggested that pollutant sources differed at the two sites. Biomass burning, resuspended dust, combustion, iron and steel industry, sea salt, secondary aerosol, and vehicle exhaust were identified at the DSL site by Positive Matrix Factorization (PMF). Secondary aerosol and vehicle exhaust accounted for 45.7% of PM<sub>2.5</sub> mass, followed 11.2%–13.7% each by industry, resuspended dust, and coal and oil combustion.

© 2018 Elsevier B.V. All rights reserved.

\* Correspondence authors.

E-mail addresses: [ceslee@polyu.edu.hk](mailto:ceslee@polyu.edu.hk) (S. Lee), [qingyanf@semc.gov.cn](mailto:qingyanf@semc.gov.cn) (Q. Fu).

## 1. Introduction

As a leading voice in China's efforts to improve air quality, Shanghai government has enhanced air quality management to reduce air pollution. The “Clean Air Action of Shanghai Municipality (2013–2017)” (Shanghai Municipal Government, 2013) was initiated only one month after the implementation of state Air Pollution Prevention and Control Action Plan (The State Council of the People's Republic of China, 2013). Coal-free zones were established in the metropolitan region (i.e., Inner Ring Road) where coal and heavy oil-fired boilers were replaced with clean energy boilers by 2015. In 2014, key industries (e.g., power plant, iron and steel, cement and flat glass industries) in Yangtze River Delta (YRD) region (Shanghai Environmental Protection Bureau, 2014) were subjected to either initiate control measures or retrofit existing desulfurization, denitration, and dust removal facilities. Industrial emission standards (i.e., smoke and dust  $\leq 10$  mg/m<sup>3</sup>, SO<sub>2</sub>  $\leq 35$  mg/m<sup>3</sup>, and NO<sub>2</sub>  $\leq 50$  mg/m<sup>3</sup>) are expected to be attained prior to the 2020 target schedule. Implementation of vehicle (i.e., gasoline and diesel) emission standards has been established in 2014 with complete implementation in 2016. Efforts have also been made to promote low/zero-emission electric vehicles. (Bureau of Statistics of Shanghai, 2014, 2015, 2016; Clean Air Asia, 2017).

Reductions in PM<sub>2.5</sub> and O<sub>3</sub> are not apparent over the last three years. As shown in the 2014–2016 Air Quality Index (AQI) report (see also in Fig. S1) (Shanghai Environmental Monitoring Center, 2017), high frequency of pollution in the number of non-attainment days is wholly attributed to the elevated PM<sub>2.5</sub> and O<sub>3</sub> concentrations, similar to other representative mega-cities in China (Ministry of Environmental Protection of China, 2016). The days that O<sub>3</sub> as the major pollutant already outnumbered PM<sub>10</sub>, making it second status

only to PM<sub>2.5</sub> in Beijing–Tianjin–Hebei (Jing–Jin–Ji) region (Wang et al., 2017; Wang et al., 2015). O<sub>3</sub> pollution becomes the primary issue in Pearl River Delta (PRD) region (Ling et al., 2017; Wang et al., 2016).

Hangzhou, the capital city of Zhejiang Province, hosted the eleventh international forum for the 20 governments and central bank governors (the G20 summit) on 9/4–9/5 in 2016, which became China's biggest diplomatic event of the year. The neighboring Shanghai, 175 km northwest of Hangzhou, initiated a “G20 Blue” program over the 14-day period from 8/24 to 9/6 with stringent pollution control measures (Shanghai Environmental Protection Bureau, 2016). As shown in Table S1, the 14-day control measures include the company shutdown or curtail 255 oil refinery, petrochemical, steel and other industries; reduce 30% of coal-fired boilers and other combustion facilities; stop 101 large construction activities; ban single-hull ferry boats and non-road machinery operations; restrict driving of high emitter (i.e., yellow-label) vehicles to downtown; extend public transport services and encourage flexible working schedules. These immediate control actions resulted in a record of low PM<sub>2.5</sub> concentration (10.6  $\mu\text{g}/\text{m}^3$ ) in the city center.

The “G20 Blue” program provides the opportunity to investigate changes in air pollutant emissions and ambient air concentrations and compositions. Here, the continuous 14-day (8/24–9/6) sampling and analysis of ground-based meteorology, criteria air pollutant concentrations (PM<sub>2.5</sub>, SO<sub>2</sub>, NO, NO<sub>2</sub>, and O<sub>3</sub>), as well as PM<sub>2.5</sub> chemical speciation were conducted at two Supersites in Shanghai, i.e., urban Pudong site (PD) and Dianshan Lake regional site (DSL). The effectiveness of the implementation of the stringent pollution control measures was evaluated during the same 14-day period from 2014 to 2016. Changes in source apportionment of PM<sub>2.5</sub> mass were analyzed among the three years.

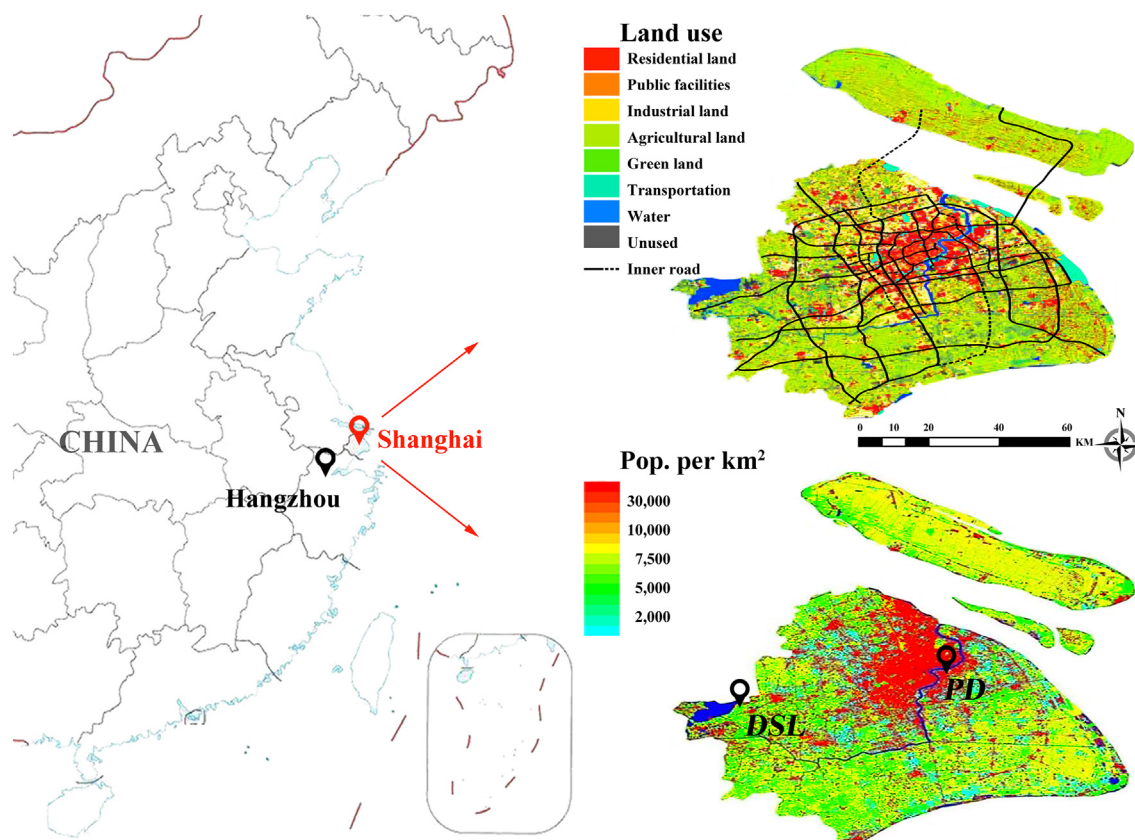


Fig. 1. Locations of the Pudong (PD) and Dianshan Lake (DSL) Supersites in Shanghai. The contour of land use and population density adopted from Shanghai statistical yearbook in 2015 (Bureau of Statistics of Shanghai, 2016).

2. Materials and methods

2.1. Supersite characteristics

The two Supersites (i.e., PD and DSL in Fig. 1), operated by the Shanghai Environmental Monitoring Center, are situated

approximately 44 km apart and designed to characterize urban exposure and pollution transport. The urban-scale PD site (31°13'N, 121°32'E) is located in downtown Shanghai (5 km east of urban center, the People's Square); whereas the DSL regional site (31°08'N, 121°05'E) is situated in 7 km east of Dianshan Lake, adjacent to Zhejiang and Jiangsu Provinces.

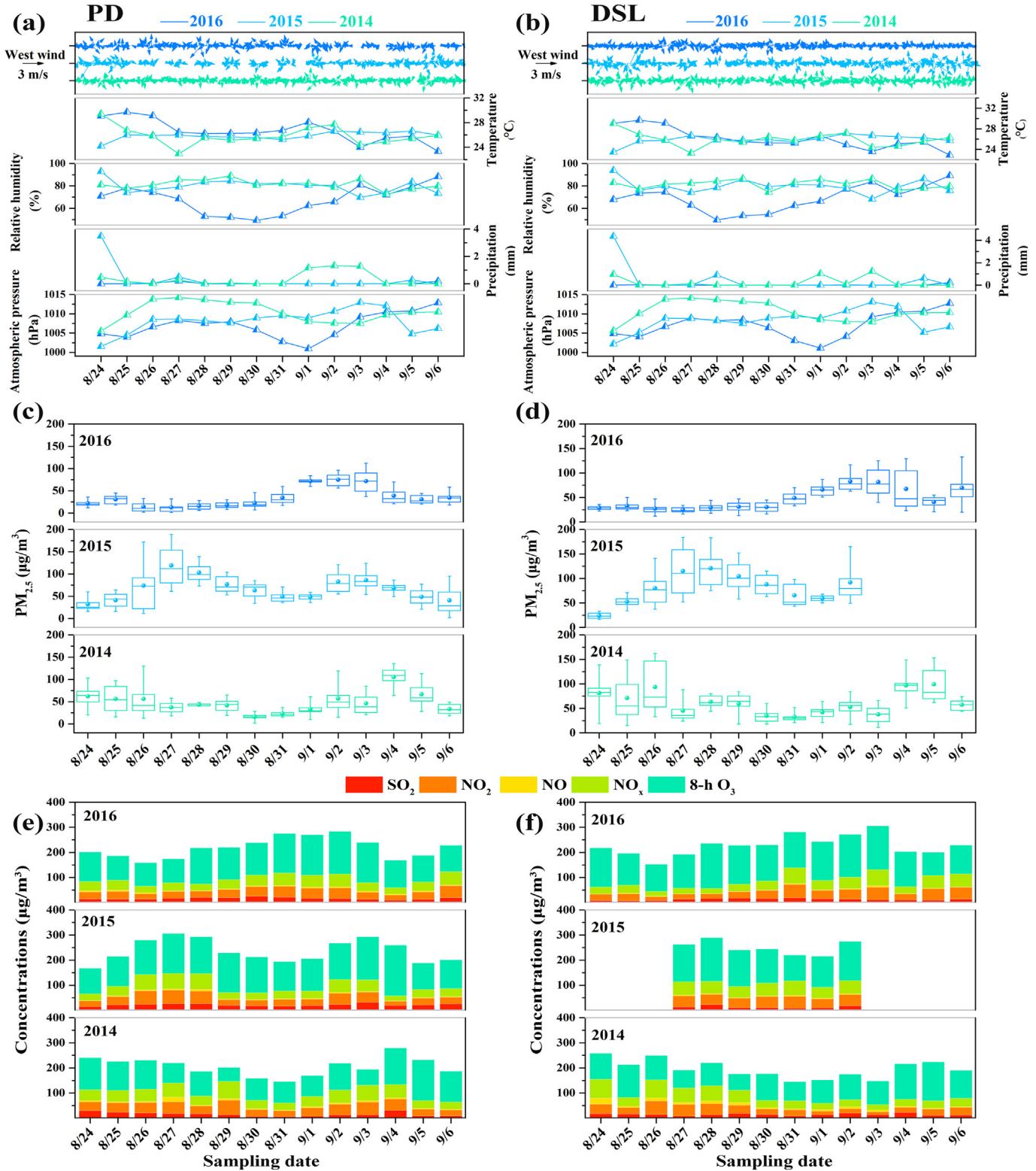


Fig. 2. Comparison of meteorological parameters, PM<sub>2.5</sub> concentrations (Box-and-Whisker Plot), and trace gaseous pollutants at the PD (a, c, and e) and DSL (b, d, and f) sites during the same period (8/24–9/6) from 2014 to 2016. A Box-and-Whisker plot: the mean (a black sphere), the median (a horizontal line in the box), the 25th percentile (the bottom edge of the box), the 75th percentile (represented by the top edge of the box), the minimum (the bottom edge of the whisker) and the maximum (the top edge of the whisker).

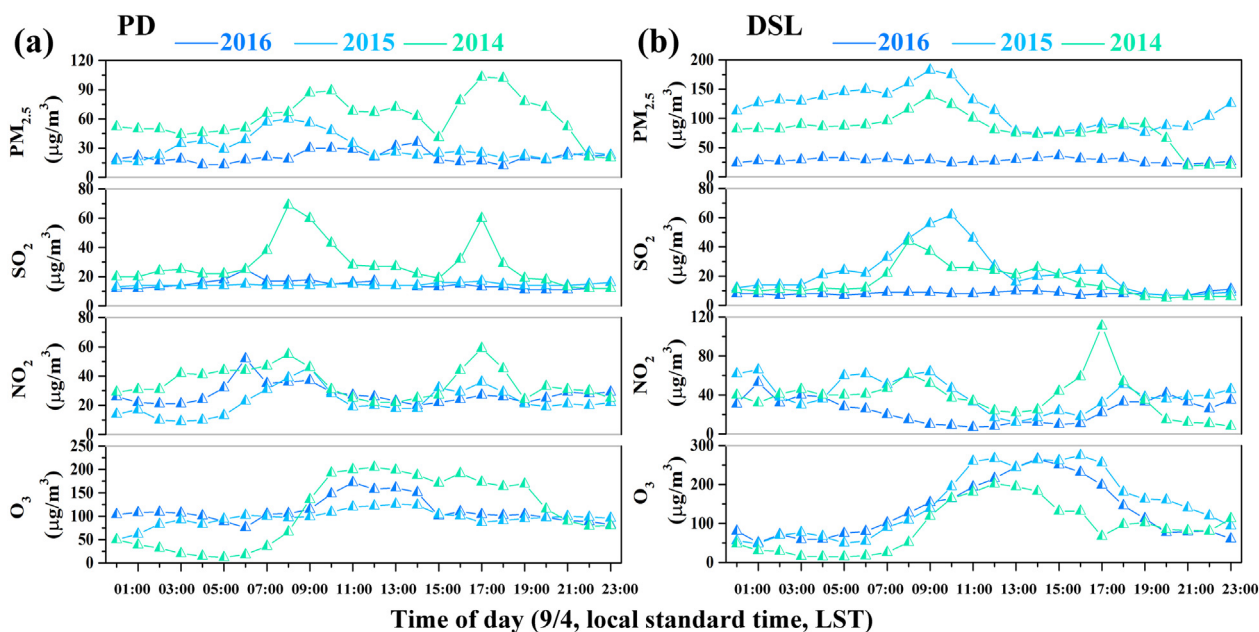


Fig. 3. Diurnal variations of  $PM_{2.5}$ ,  $SO_2$ ,  $NO_2$ , and  $O_3$  at the PD (a) and DSL (b) sites on 9/4 from 2014 to 2016.

## 2.2. Samples collection and analysis

$PM_{2.5}$  mass concentrations were determined by a tapered-element oscillating microbalance monitor (TEOM, Thermo FH62C-14). 24-h  $PM_{2.5}$  samples were collected on quartz-fiber filters (Tissuquartz 2600 QAT, Pallflex membrane filters, USA), using a high-volume sampler (Guangzhou Mingye Huanbao Technology Company, China) with a flow rate of  $1.0 \text{ m}^3/\text{h}$ . The quartz-fiber filters were equilibrated at a constant temperature ( $20 \pm 1^\circ \text{C}$ ) and relative humidity ( $40 \pm 1\%$ ) environment for 24 h before weighing. Gravimetric analyses were conducted using an analytical balance (Mettler Toledo, Switzerland) with a precision of  $10 \mu\text{g}$ . Detailed quality control/quality assurance (QC/QA) has been described in the literature (Chow et al., 2015; Collett, 2016; Watson et al., 2017).

Hourly  $PM_{2.5}$  water-soluble inorganic species (i.e.,  $SO_4^{2+}$ ,  $NO_3^-$ ,  $NH_4^+$ ,  $Cl^-$ ,  $K^+$ ,  $Ca^{2+}$ ,  $Na^+$ , and  $Mg^{2+}$ ) and precursor gases (e.g.,  $SO_2$  and  $NH_3$ ) were measured by an online MARGA (Monitor for Aerosols and Gases in Ambient Air, Model ADI2080, Metrohm Applikon BV). The MARGA system consists of a steam-jet aerosol collector with a  $PM_{2.5}$  inlet where gases were removed by a wet rotating denuder and ions were captured and dissolved into the supersaturated stream before analyzed by ion chromatograph (Chow and Watson, 2017). Organic and elemental carbon (OC and EC) were acquired with an RT-4 analyzer (Sunset Lab, USA). A total of 16 trace elements (i.e., Fe, V, Cr, Mn, Co, Ni, Cu, Zn, Ga, Ge, As, Se, Cd, Au, Ba, Pb) was monitored by a continuous multi-metals monitor (Cooper Xact625) equipped with a reel-to-reel filter tape for nondestructive energy-dispersive X-ray fluorescence (EDXRF) analysis. Due to missing value ( $>20\%$ ) (Yuan et al., 2008) for trace elements at the PD site, 336 samples with 26 species at the DSL site were used for the Positive Matrix Factorization (PMF) analysis.

Nitrogen oxides were measured using a chemiluminescence  $NO-NO_2-NO_x$  analyzer (EC 9841B) with a minimum detection limit of  $0.4 \times 10^{-9}$  (volume fraction), while  $O_3$  were monitored using a UV spectrophotometry ozone analyzer (EC 9810B) with a minimum detection limit of  $0.4 \times 10^{-9}$ . Meteorological parameters including wind speed and direction, temperature, relative humidity, pressure, and rainfall were monitored by an automatic meteorological station (Met Station One Instrument, USA), which are placed 18 m above the ground level on the rooftop of each Supersite. These measurements follow the QC/QA

procedure specified in the Technical Guideline of Automatic Stations of Ambient Air Quality in Shanghai, which is based on the national specification HJ/T193–2005 (Ministry of Environmental Protection of China, 2005) and HJ/193–2013 (Ministry of Environmental Protection of China, 2013).

## 3. Results and discussion

### 3.1. Meteorological conditions and atmospheric pollutant concentrations

Fig. 2a–b show that the daily meteorological phenomena were similar among the three years with a few exception. Temperatures remained moderate ( $26.8^\circ \text{C}$ ) with low average relative humidity (74%) except for the period of 8/28–8/30 in 2016. Atmospheric pressures were lower during 8/29–9/1 in 2016. Wind speed was remaining low, averaging 1.9 m/s, consistent with the 168-h back trajectories (see also in Fig. S2). The predominant northwesterly winds from 2014 to 2016 were 50.3%, 47.4%, and 44.1% at the PD site, and 48.8%, 41.6%, and 43.5% at the DSL site, respectively. Therefore, meteorological conditions during the 2016 G20 period were not atypical, indicating that comparisons of air pollutant concentrations can be made among the three years.

In the autumn harvest period, biomass burning can emit  $>60\%$  of trace gases and particles emissions in the YRD region (Zha et al., 2013). Hence, Shanghai usually suffers from the greater impact of the pollutant transport from its adjacent Provinces. More abundant active fires still existed in 2016 from the neighboring regions which somewhat affect the pollution condition in Shanghai (see also in Fig. S3).

Fig. 2c–d show higher reductions in  $PM_{2.5}$  during the 2016 G20 period. Daily  $PM_{2.5}$  concentrations during 8/24–8/31 were low, averaging  $24.0 \mu\text{g}/\text{m}^3$  with a minimum of  $10.6 \mu\text{g}/\text{m}^3$  at PD, about 61.0% and 40.8% lower than these found in 2015 and 2014, respectively. Lower  $PM_{2.5}$  concentrations were also found for the DSL site during the last week of August in 2016, averaging  $31.2 \mu\text{g}/\text{m}^3$  with a minimum of  $16.0 \mu\text{g}/\text{m}^3$ , about 66.0% and 48.6% lower than 2015 and 2014, respectively. The prevailing northwesterly winds enhanced the diffusion of air pollutants. Prior to the commencement of G20 (9/2–9/3),  $PM_{2.5}$  concentrations increased to  $74.8 \mu\text{g}/\text{m}^3$  at PD and  $81.6 \mu\text{g}/\text{m}^3$  at DSL with some decreases on 9/4–9/6 in 2016. The DSL regional site, is surrounded with green and agricultural lands in Fig. 1, suffered pollutant transport from

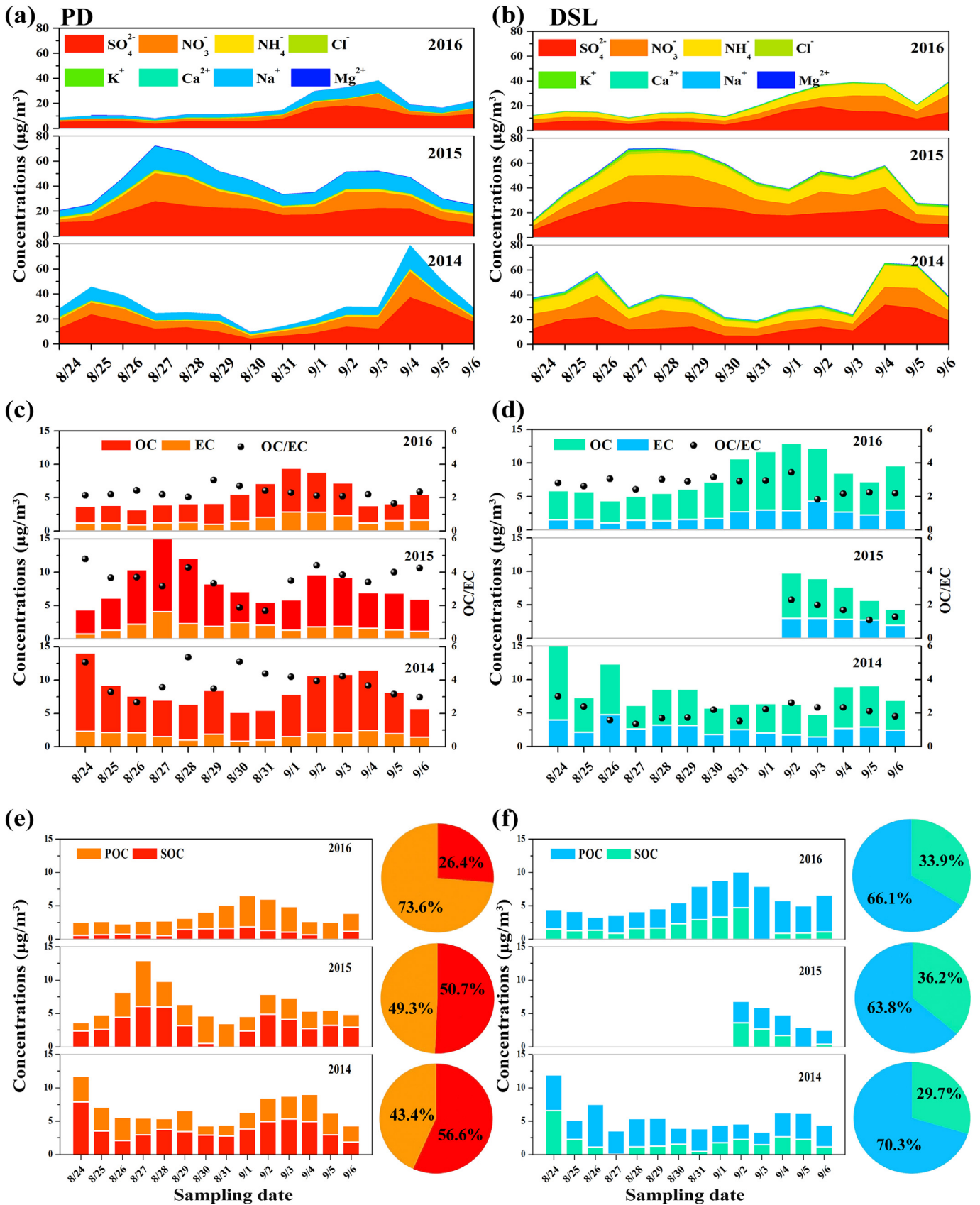


**Fig. 4.** Comparison of water-soluble inorganic ions (WSIIs) (a and b), carbonaceous species (c and d), and SOC estimation (e and f) in  $\text{PM}_{2.5}$  at the PD and DSL sites during the same period (8/24–9/6) from 2014 to 2016. Pie charts (inset of e and f): changes in the fractions of POC and SOC in OC concentrations at both sites.

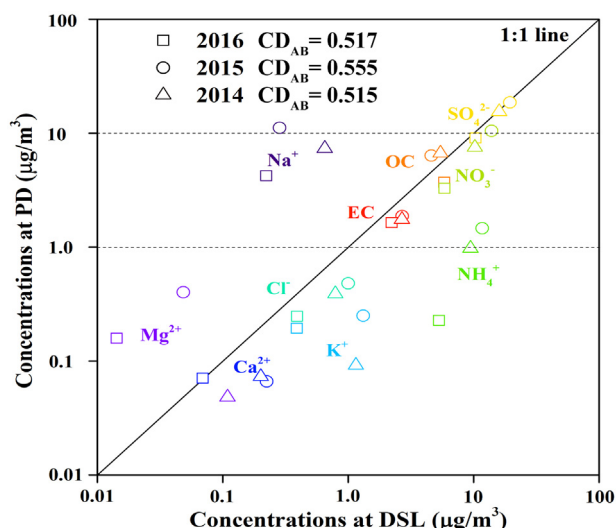


Fig. 5. Coefficient of divergence (CD) that characterizes the differences of PM<sub>2.5</sub> chemical components between PD and DSL during the same period (8/24–9/6) from 2014 to 2016.

the neighboring regions with clockwise transport from northwesterly to northeasterly (see also in Fig. S2), contributing to a rise of pollutant concentrations.

Gaseous comparison excluded CO as CO concentrations remain below the Chinese National Ambient Air Quality Standards (NAAQS) in recent years (Clean Air Asia, 2017). Not many changes in annual SO<sub>2</sub> concentrations ranged from 18.9 µg/m<sup>3</sup> in 2014 to 15.9 µg/m<sup>3</sup> in 2016, below the NAAQS First Standard of 20 µg/m<sup>3</sup>. Annual NO<sub>2</sub> concentrations ranged from 42.1 µg/m<sup>3</sup> in 2014 to 40.6 µg/m<sup>3</sup> in 2016, close to the NAAQS of 40 µg/m<sup>3</sup>. Consequently, no apparent changes in SO<sub>2</sub> were found during the same 14-day from 2014 to 2016 in Fig. 2e–f, with an average of 15.1 µg/m<sup>3</sup> in 2014, 21.8 µg/m<sup>3</sup> in 2015, and 16.6 µg/m<sup>3</sup> in 2016 at the PD site and 14.3 µg/m<sup>3</sup> in 2014, 13.0 µg/m<sup>3</sup> in 2015, and 12.8 µg/m<sup>3</sup> in 2016 at the DSL site. Due to regional transport by the prevailing northwesterly winds, concentrations of SO<sub>2</sub> at PD were slightly higher than DSL, while NO<sub>2</sub> at PD was 9.4% higher than that at DSL, reflecting the impact of motor vehicle emissions in urban areas.

On the contrary, concentrations of 8-h O<sub>3</sub> elevated to higher instead of dropping during the G20 period, with higher increases found at the PD site as compared to DSL. This is consistent with those reported in recent studies (Li et al., 2018; Wang et al., 2015; Zhao et al., 2018), where inhibition of NO<sub>x</sub> on O<sub>3</sub> was more significant in urban areas.

The diurnal variations on 9/4 (the first day of the 2016 G20 summit) of air pollutants were compared in Fig. 3. It is obvious that rush-hour peaks for PM<sub>2.5</sub>, SO<sub>2</sub>, and NO<sub>2</sub> found in 2014 and 2015 were diminished in 2016. PM<sub>2.5</sub> and SO<sub>2</sub> concentrations remained low throughout the day at the PD and DSL sites. Different diurnal patterns were found for NO<sub>2</sub>, peaked at 07:00 and 18:00 LST during the rush-hour traffic at the PD site but remained relatively lower (<40 µg/m<sup>3</sup>) at the DSL site with accommodation found during late evening (23:00 LST) to early morning (02:00 LST). Concentrations of ground level O<sub>3</sub> were affected by temperature, namely, high temperature in the daytime was favorable for O<sub>3</sub> formation (Xue et al., 2014). Diurnal curves of all monitored pollutants except for O<sub>3</sub> in the G20 period were lower than those found in the previous two years.

### 3.2. Changes in chemical composition of PM<sub>2.5</sub>

#### 3.2.1. Water-soluble inorganic ions and carbonaceous species

In Fig. 4a–b, concentrations of chemical composition of PM<sub>2.5</sub> decreased during the 14-day period in 2016 and their reductions varied between the PD and DSL sites. Total water-soluble inorganic ions

(TWSIIs) concentrations averaged 9.69 µg/m<sup>3</sup> at PD and 13.0 µg/m<sup>3</sup> at DSL, which accounted for 56.2% and 52.3% of PM<sub>2.5</sub> mass in the G20 period (see also in Fig. S4). Compared with the previous two years, TWSIIs decreased by an average of 57.5% and 44.0% at PD and DSL, respectively. As for main secondary ionic aerosols (SIA), sulfate SO<sub>4</sub><sup>2-</sup>, nitrate NO<sub>3</sub><sup>-</sup>, and ammonium NH<sub>4</sub><sup>+</sup> (SNA), averagely 41.5%, 68.8%, and 76.5% of reductions were attained at PD and just 28.9%, 29.5%, and 26.0% at DSL. SNA shared 88.3% of TWSIIs at PD and 86.8% at DSL among the three years. Strong correlations between SIA and PM<sub>2.5</sub> were observed at the PD (R = 0.87, n = 336, p < 0.01) and DSL (R = 0.82, n = 336, p < 0.01) sites, respectively. These findings denoted that NO<sub>3</sub><sup>-</sup>, SO<sub>4</sub><sup>2-</sup> and NH<sub>4</sub><sup>+</sup> were the major ions in PM<sub>2.5</sub> and SIA variations were associated with the formation, transportation and removal of PM<sub>2.5</sub>.

No massive reduction in K<sup>+</sup> concentrations was at the PD site from 0.25 µg/m<sup>3</sup> to 0.19 µg/m<sup>3</sup>; whereas banning burning activities contributed to up to 89.6% reductions at the DSL site. Fig. 4b shows apparent reduction of 44.2% for NH<sub>4</sub><sup>+</sup> at the DSL site, suggesting the effectiveness of precursor NH<sub>3</sub> emissions control from agricultural activities (Xu et al., 2015; Zhang et al., 2018). However, NH<sub>4</sub><sup>+</sup> exists in compound form through the combination of SO<sub>4</sub><sup>2-</sup> and NO<sub>3</sub><sup>-</sup>. It is possible that the reductions of SO<sub>4</sub><sup>2-</sup> and NO<sub>3</sub><sup>-</sup> are associated with the NH<sub>4</sub><sup>+</sup> decreases (Collett, 2016; Zhang et al., 2018) in the urban environment and the higher concentrations of NH<sub>4</sub><sup>+</sup> at the regional DSL are complicated rather than singly from the local.

Na<sup>+</sup> concentrations at the PD site were 5 times higher than those at DSL, implying the impact from sea salt at the urban site in Shanghai (Qiao et al., 2016). Reductions of Na<sup>+</sup>, Ca<sup>2+</sup>, and Mg<sup>2+</sup> corresponded to dust controls in construction activities and steel sweeping (Xiu et al., 2004; Zhang et al., 2015). Water soluble Ca<sup>2+</sup> accounted for 1.7% to 2.0% of TWSIIs, lower than the 6.8% in Wuhan (Zhang et al., 2015), 4.0% in Zhengzhou (Geng et al., 2013), and 2.6% in Xiamen (Zhang et al., 2012). Weak correlations were found for Ca<sup>2+</sup> between the PD and DSL sites (R = 0.28, n = 336, p < 0.05), suggesting differences in geological composition between the urban and regional areas. Yang et al. (2018) reports high Cl<sup>-</sup>/Na<sup>+</sup> ratios (2.46–5.0) in northern and western China. These ratios were about an order of magnitude higher than those found at PD (0.44) but similar to 2.31 found at DSL. The lower Cl<sup>-</sup>/Na<sup>+</sup> ratio at PD could be ascribed by curtailing coal-oriented consumptions in urban Shanghai (He et al., 2001).

Carbonaceous aerosol (TC) is the major component of PM<sub>2.5</sub> and consists of two components, i.e., organic carbon (OC) and elemental carbon (EC). OC could be divided into primary organic carbon (POC) and secondary organic carbon (SOC). POC is emitted directly in the particle-phase and SOC is formed from gas-to-particle conversion in the atmosphere. The presence of SOC can be estimated by the minimum OC/EC ratio (Huang et al., 2012; Zhang et al., 2012):

$$POC = EC \times \left( \frac{OC}{EC} \right)_{\min} \quad (1)$$

$$SOC = OC - POC \quad (2)$$

where (OC/EC)<sub>min</sub> is the minimum OC/EC ratio. The concentrations of OC (POC and SOC) and EC, as well as OC/EC ratios of PM<sub>2.5</sub> at the PD and DSL sites are illustrated in Fig. 4c–f. Average TC concentrations were 3.51 µg/m<sup>3</sup> and 6.03 µg/m<sup>3</sup> during the 14-day period in 2016 and accounted for 14.5% and 19.3% of PM<sub>2.5</sub> mass (see also in Fig. S4) at PD and DSL, respectively. OC accounted for 71.0%–77.2% of TC, ranging from 7.13 µg/m<sup>3</sup> to 7.39 µg/m<sup>3</sup> at PD and 1.85 µg/m<sup>3</sup> to 2.19 µg/m<sup>3</sup> at DSL during the same 14-day period from 2014 to 2016.

Good correlations were found between OC and K<sup>+</sup> (R = 0.97, n = 336, p < 0.01) at the DSL site, suggesting their common emission sources (Li et al., 2015) and the association with fire events (see also in Fig. S3). In Fig. 4c–d, average OC/EC ratios decreased from 3.9 in 2014, 3.6 in 2015 to 2.2 in 2016 at the PD site, more pronounced than those found at the DSL site from 2.7 in 2014 to 2.1 in 2016. In Fig. 4e–f, average

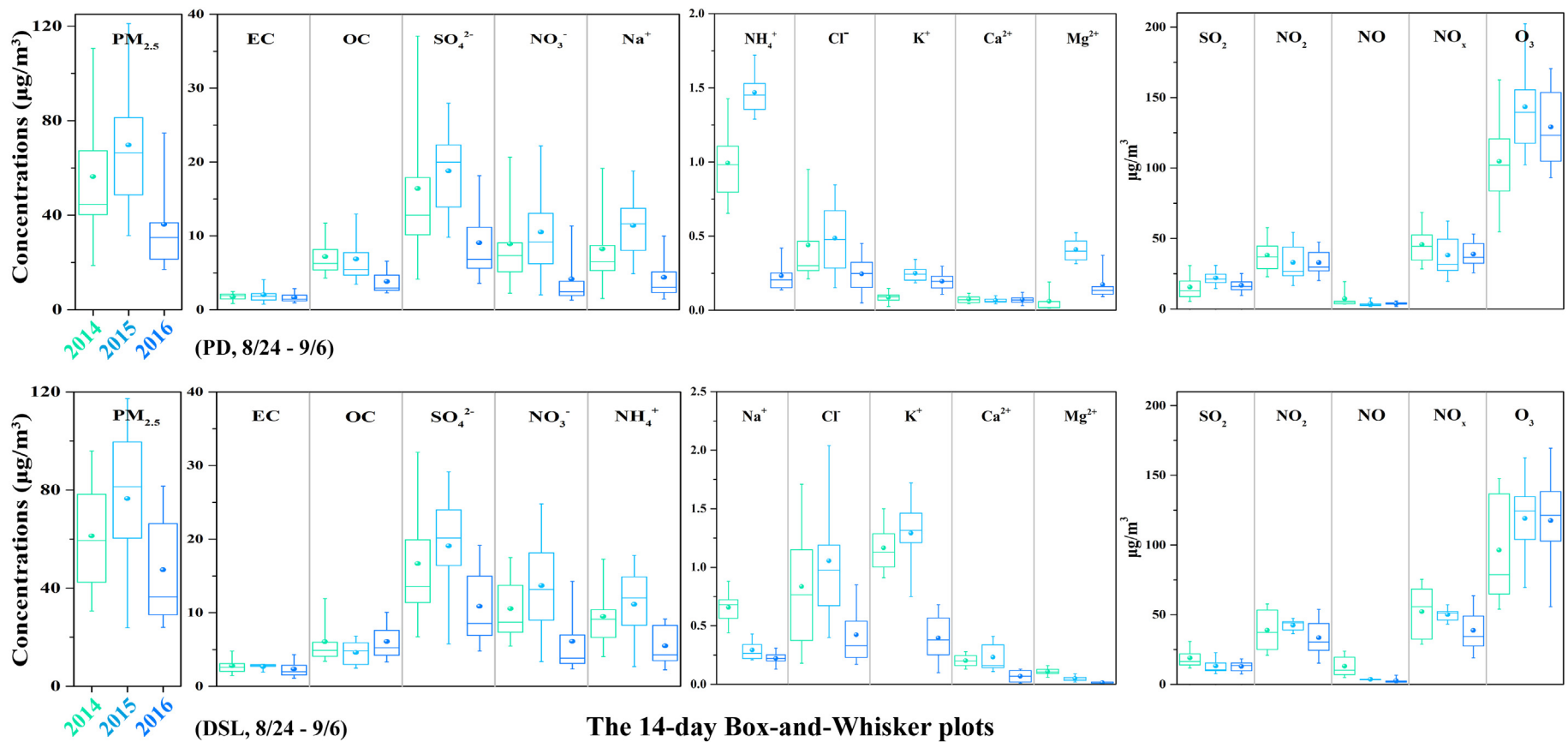


Fig. 6. Comparison of concentrations of air pollutants (PM<sub>2.5</sub> mass, carbon, ions and trace gaseous pollutants) at the PD (a) and DSL (b) sites during the same period (8/24–9/6) from 2014 to 2016.

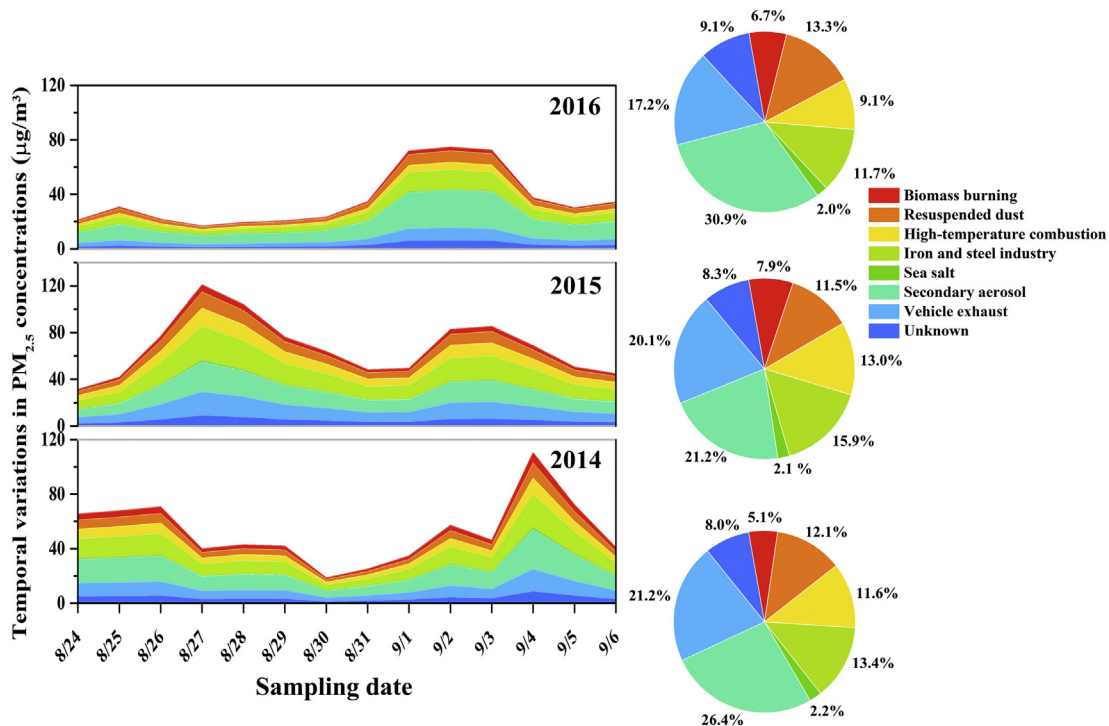


Fig. 7. Changes in source apportionment resolved from  $PM_{2.5}$  samples at the DSL site during the same period (8/24–9/6) from 2014 to 2016.

SOC during the G20 period were  $2.7 \mu\text{g}/\text{m}^3$  and  $3.6 \mu\text{g}/\text{m}^3$ , accounted for 26.4% and 33.9% of OC at the PD and DSL sites, respectively. The SOC/OC ratios shared fewer variations at DSL (29.7% to 36.2%) than PD (26.4% to 56.6%).  $PM_{2.5}$  shows higher correlations with SOC ( $R = 0.85$ ,  $n = 336$ ,  $p < 0.01$ ) at PD and ( $R = 0.75$ ,  $n = 336$ ,  $p < 0.01$ ) at DSL than with POC ( $R = 0.53$ ,  $n = 60$ ,  $p < 0.01$ ) at PD and ( $R = 0.66$ ,  $n = 336$ ,  $p < 0.01$ ) at DSL. These findings reflect that organic components in the atmosphere were related to the formation, transportation and removal of  $PM_{2.5}$  in Shanghai (Huang et al., 2012; Liang et al., 2016). Large reductions in SOC/OC ratios at the PD site during the G20 period were more pronounced than those found at DSL. Weak correlations between OC and EC ( $R = 0.32$ ,  $n = 336$ ,  $p < 0.05$ ) at PD and ( $R = 0.28$ ,  $n = 336$ ,  $p < 0.05$ ) at DSL indicate that they derived from different sources (Li et al., 2012; Tao et al., 2014).

### 3.2.2. Divergence analysis between two sites

Coefficient of divergence (CD) can be utilized to characterize the differences of chemical components between the two sampling sites, calculated by the following equation (Zhang and Friedlander, 2000):

$$CD_{AB} = \sqrt{\frac{1}{n} \sum_{i=1}^n \left( \frac{C_{iA} - C_{iB}}{C_{iA} + C_{iB}} \right)^2} \quad (3)$$

where  $C_{iA}$  and  $C_{iB}$  represent the concentrations of component  $i$  at site A and site B, respectively. If the CD is approximate to 0.00, the emission sources between the two sites are similar; whereas close to 1.00, the two sites are different (Zhang and Friedlander, 2000). This approach was adopted by (Yang et al., 2002) in Beijing ( $CD = 0.064$ ) and (Zhang et al., 2015) in Wuhan ( $CD = 0.098$ ), indicating that the similarity of  $PM_{2.5}$  compositions. In contrast, the values of CDs between PD and DSL ranged 0.52–0.56 from 2014 to 2016 as shown in Fig. 5., which supports the investigation of the complicated impacts between urban and regional sites.

## 4. Effectiveness of the pollution control measures

Annual mean concentrations of  $PM_{2.5}$ ,  $SO_2$ , and  $NO_2$  reduced by 14.1%, 21.9%, and 11.4%, respectively, in 2016 as compared to 2014 and 2015. Though the 14-day pollution control measures imposed during the G20 period, concentrations of  $PM_{2.5}$  mass, carbon, and ions (especially  $SO_4^{2-}$ ,  $NO_3^-$ , and  $NH_4^+$ ) decreased significantly as compared to the same period in the previous two years shown in Fig. 6. Higher number of the air quality attainment days were achieved (see also in Fig. S5). No improvement was found for  $O_3$  at either the PD or DSL sites.

Seven sources were identified by the Positive Matrix Factorization (PMF) model (see also in Fig. S6) for  $PM_{2.5}$  samples at the DSL site, including biomass burning, resuspended dust, high-temperature combustion, iron and steel industry, sea salt, secondary aerosol, and vehicle exhaust. Fig. 7 shows changes in temporal variations in  $PM_{2.5}$  and source contribution among the three years. The two largest contributors were secondary aerosols and vehicle exhaust among the three years, which accounted for 45.7% of  $PM_{2.5}$  mass, followed by iron and steel industry (13.7%), resuspended dust (12.3%), and high-temperature combustion from coal and oil boilers (11.2%). Biomass burning ranged from 5.1% to 7.9% of  $PM_{2.5}$  and was attributed to the prevailing northwesterly transports, also supported by the back trajectories (see also in Fig. S2) and active fire detections (see also in Fig. S3).

## 5. Conclusions

Implementation of stringent pollution control measures over the 14-day period resulted in large reduction in pollution concentrations. The effectiveness of the pollution control in the urban center was more pronounced than regional areas. If the onset of unfavorable meteorological conditions is forecasted, the enhanced reduction measures would be implemented several days ahead of pollution episodes. Since the impact of multiple pollutants on  $PM_{2.5}$  and  $O_3$  concentrations and atmospheric oxidation capacity is nonlinear and complicated, reduction in precursor gases (e.g.,  $SO_2$ ,  $NO_x$ ,  $NH_3$  and VOCs) should be synergistically strengthened for the next stage. However, its long-term impacts on ambient

concentration levels need to be further evaluated. A market-based approach needs to be examined to evaluate the cost of an ad-hoc closures of industries. The profit and loss between the environment and business need to be balanced.

## Notes

The authors declare no competing financial interest.

## Acknowledgements

This research was financially supported by The Ministry of Science and Technology, China (2013FY112700 and 2014BAC22B07), Science and Technology Commission of Shanghai (Project No. 14DZ1202900), The Research Grants Council of Hong Kong Government (Project No. T24/504/17), The Research Grants Council of Hong Kong Government (PolyU152083/14E and PolyU152090/15E), and Hong Kong RGC Collaborative Research Fund (C5022–14G).

## Appendix A. Supplementary data

Supplementary Information associated with this article can be found in this section, including: 14-day pollution control measures, distribution of Air Quality Index (AQI) in Shanghai from 2014 to 2016, NOAA HYSPLIT trajectory model results, active fire detection in neighboring regions, fractional abundance of five major species of PM<sub>2.5</sub>, changes in air quality attainment during the G20 period, and source identification PM<sub>2.5</sub> samples using PMF model. Supplementary data to this article can be found online at doi:<https://doi.org/10.1016/j.scitotenv.2018.08.219>.

## References

- Bureau of Statistics of Shanghai (BBS), 2014. Shanghai Statistical Yearbook 2013. China Statistics Press, Beijing (in Chinese).
- Bureau of Statistics of Shanghai (BBS), 2015. Shanghai Statistical Yearbook 2014. China Statistics Press, Beijing (in Chinese).
- Bureau of Statistics of Shanghai (BBS), 2016. Shanghai Statistical Yearbook 2015. China Statistics Press, Beijing (in Chinese).
- Chow, J.C., Watson, J.G., 2017. Enhanced ion chromatographic speciation of water-soluble PM<sub>2.5</sub> to improve aerosol source apportionment. *Aerosol Sci. Eng.* 1, 7–24.
- Chow, J.C., Wang, X., Sumlin, B.J., Gronstal, S.B., Chen, L.-W.A., Trimble, D.L., Kohl, S.D., Mayorga, S.R., Riggio, G., Hurbain, P.R., 2015. Optical calibration and equivalence of a multiwavelength thermal/optical carbon analyzer. *Aerosol Air Qual. Res.* 15, 1145.
- Clean Air Asia (CAA), 2017. China Air 2016–Air Pollution Prevention and Control Progress in Chinese Cities.
- Collett, J.L., 2016. The importance of vehicle emissions as a source of atmospheric ammonia in the megacity of Shanghai. *Atmos. Chem. Phys.* 16, 3577.
- Geng, N., Wang, J., Xu, Y., Zhang, W., Chen, C., Zhang, R., 2013. PM<sub>2.5</sub> in an industrial district of Zhengzhou, China: chemical composition and source apportionment. *Particuology* 11, 99–109.
- He, K., Yang, F., Ma, Y., Zhang, Q., Yao, X., Chan, C.K., Cadle, S., Chan, T., Mulawa, P., 2001. The characteristics of PM<sub>2.5</sub> in Beijing, China. *Atmos. Environ.* 35, 4959–4970.
- Huang, H., Ho, K., Lee, S., Tsang, P., Ho, S.S.H., Zou, C., Zou, S., Cao, J., Xu, H., 2012. Characteristics of carbonaceous aerosol in PM<sub>2.5</sub>: Pearl Delta river region, China. *Atmos. Res.* 104, 227–236.
- Li, Y.-C., Yu, J.Z., Ho, S.S.H., Yuan, Z., Lau, A.K., Huang, X.-F., 2012. Chemical characteristics of PM<sub>2.5</sub> and organic aerosol source analysis during cold front episodes in Hong Kong, China. *Atmos. Res.* 118, 41–51.
- Li, B., Zhang, J., Zhao, Y., Yuan, S., Zhao, Q., Shen, G., Wu, H., 2015. Seasonal variation of urban carbonaceous aerosols in a typical city Nanjing in Yangtze River Delta, China. *Atmos. Environ.* 106, 223–231.
- Li, Z., Xue, L., Yang, X., Zha, Q., Tham, Y.J., Yan, C., Louie, P.K., Luk, C.W., Wang, T., Wang, W., 2018. Oxidizing capacity of the rural atmosphere in Hong Kong, Southern China. *Sci. Total Environ.* 612, 1114–1122.
- Liang, C.-S., Duan, F.-K., He, K.-B., Ma, Y.-L., 2016. Review on recent progress in observations, source identifications and countermeasures of PM<sub>2.5</sub>. *Environ. Int.* 86, 150–170.
- Ling, Z., Zhao, J., Fan, S., Wang, X., 2017. Sources of formaldehyde and their contributions to photochemical O<sub>3</sub> formation at an urban site in the Pearl River Delta, southern China. *Chemosphere* 168, 1293–1301.
- Ministry of Environmental Protection of China (MEP), 2005. Automated Methods for Ambient Air Quality Monitoring (HJ/T193–2005).
- Ministry of Environmental Protection of China (MEP), 2013. Technical Specifications for Installation and Acceptance of Ambient Air Quality Continuous Automated Monitoring System for SO<sub>2</sub>, NO<sub>2</sub>, O<sub>3</sub> and CO (HJ193–2013).
- Ministry of Environmental Protection of China (MEP), 2016. Urban Ambient Air Quality Daily Report. <http://www.mep.gov.cn/hjzl/> (in Chinese).
- Qiao, T., Zhao, M., Xiu, G., Yu, J., 2016. Simultaneous monitoring and compositions analysis of PM<sub>1</sub> and PM<sub>2.5</sub> in Shanghai: implications for characterization of haze pollution and source apportionment. *Sci. Total Environ.* 557, 386–394.
- Shanghai Environmental Monitoring Center (SEMC), 2017. Real-time Air Quality Reporting System in Shanghai.
- Shanghai Environmental Protection Bureau (SEPB), 2014. Air Pollution Prevention and Control Plan for Key Industries in Yangtze River Delta.
- Shanghai Environmental Protection Bureau (SEPB), 2016. The G20 Air Pollution Control Program in Shanghai (in Chinese).
- Shanghai Municipal Government (SMG), 2013. Clean Air Action of Shanghai Municipality (2013–2017) (in Chinese).
- Tao, J., Gao, J., Zhang, L., Zhang, R., Che, H., Zhang, Z., Lin, Z., Jing, J., Cao, J., Hsu, S.-C., 2014. PM<sub>2.5</sub> pollution in a megacity of southwest China: source apportionment and implication. *Atmos. Chem. Phys.* 14, 8679–8699.
- The State Council of the People's Republic of China, 2013. Air Pollution Prevention and Control Action Plan (in Chinese).
- Wang, Z., Li, Y., Chen, T., Li, L., Liu, B., Zhang, D., Sun, F., Wei, Q., Jiang, L., Pan, L., 2015. Changes in atmospheric composition during the 2014 APEC conference in Beijing. *J. Geophys. Res. Atmos.* 120, 12695–12707.
- Wang, N., Lyu, X., Deng, X., Guo, H., Deng, T., Li, Y., Yin, C., Li, F., Wang, S., 2016. Assessment of regional air quality resulting from emission control in the Pearl River Delta region, southern China. *Sci. Total Environ.* 573, 1554–1565.
- Wang, T., Xue, L., Brimblecombe, P., Lam, Y.F., Li, L., Zhang, L., 2017. Ozone pollution in China: a review of concentrations, meteorological influences, chemical precursors, and effects. *Sci. Total Environ.* 575, 1582–1596.
- Watson, J.G., Tropp, R.J., Kohl, S.D., Wang, X., Chow, J.C., 2017. Filter processing and gravimetric analysis for suspended particulate matter samples. *Aerosol Sci. Eng.* 1, 93–105.
- Xiu, G., Zhang, D., Chen, J., Huang, X., Chen, Z., Guo, H., Pan, J., 2004. Characterization of major water-soluble inorganic ions in size-fractionated particulate matters in Shanghai campus ambient air. *Atmos. Environ.* 38, 227–236.
- Xu, P., Zhang, Y., Gong, W., Hou, X., Kroeze, C., Gao, W., Luan, S., 2015. An inventory of the emission of ammonia from agricultural fertilizer application in China for 2010 and its high-resolution spatial distribution. *Atmos. Environ.* 115, 141–148.
- Xue, L., Wang, T., Louie, P.K., Luk, C.W., Blake, D.R., Xu, Z., 2014. Increasing external effects negate local efforts to control ozone air pollution: a case study of Hong Kong and implications for other Chinese cities. *Environ. Sci. Technol.* 48, 10769–10775.
- Yang, F., He, K., Ma, Y., Zhang, Q., Yao, X., Chan, C.K., Cadle, S., Chan, T., Mulawa, P., 2002. Chemical characteristics of PM<sub>2.5</sub> species in Beijing ambient air. *J. Tsinghua Univ. (Sci. Technol.)* 42, 1605–1608.
- Yang, X., Wang, T., Xia, M., Gao, X., Li, Q., Zhang, N., Gao, Y., Lee, S., Wang, X., Xue, L., 2018. Abundance and origin of fine particulate chloride in continental China. *Sci. Total Environ.* 624, 1041–1051.
- Yuan, H., Zhuang, G., Li, J., Wang, Z., Li, J., 2008. Mixing of mineral with pollution aerosols in dust season in Beijing: revealed by source apportionment study. *Atmos. Environ.* 42, 2141–2157.
- Zha, S., Zhang, S., Cheng, T., Chen, J., Huang, G., Li, X., Wang, Q., 2013. Agricultural fires and their potential impacts on regional air quality over China. *Aerosol Air Qual. Res.* 13, 992–1001.
- Zhang, Z., Friedlander, S.K., 2000. A comparative study of chemical databases for fine particle Chinese aerosols. *Environ. Sci. Technol.* 34, 4687–4694.
- Zhang, F., Xu, L., Chen, J., Yu, Y., Niu, Z., Yin, L., 2012. Chemical compositions and extinction coefficients of PM<sub>2.5</sub> in peri-urban of Xiamen, China, during June 2009–May 2010. *Atmos. Res.* 106, 150–158.
- Zhang, F., Wang, Z.-w., Cheng, H.-r., Lv, X.-p., Gong, W., Wang, X.-m., Zhang, G., 2015. Seasonal variations and chemical characteristics of PM<sub>2.5</sub> in Wuhan, central China. *Sci. Total Environ.* 518, 97–105.
- Zhang, L., Chen, Y., Zhao, Y., Henze, D.K., Zhu, L., Song, Y., Paulot, F., Liu, X., Pan, Y., Lin, Y., 2018. Agricultural ammonia emissions in China: reconciling bottom-up and top-down estimates. *Atmos. Chem. Phys.* 18, 339.
- Zhao, S., Yu, Y., Yin, D., Qin, D., He, J., Dong, L., 2018. Spatial patterns and temporal variations of six criteria air pollutants during 2015 to 2017 in the city clusters of Sichuan Basin, China. *Sci. Total Environ.* 624, 540–557.